CHINESE OPTICS LETTERS

Vol. 19, No. 7 | July 2021

Precise control of micro-rod resonator free spectral range via iterative laser annealing

Qin Wen (温 钦), Wenwen Cui (崔雯雯), Yong Geng (耿 勇)*, Heng Zhou (周 恒), and Kun Qiu (邱 昆)

Key Laboratory of Optical Fiber Sensing and Communication Networks, School of Information and Communication Engineering, University of Electronic Science and Technology of China, Chengdu 611731, China

*Corresponding author: gengyong@uestc.edu.cn

Received November 20, 2020 | Accepted December 18, 2020 | Posted Online April 8, 2021

We demonstrate a novel method to control the free spectral range (FSR) of silica micro-rod resonators precisely. This method is accomplished by iteratively applying laser annealing on the already-fabricated micro-rod resonators. Fine and repeatable increasing of resonator FSR is demonstrated, and the best resolution is smaller than 5 MHz, while the resonator quality-factor is only slightly affected by the iterative annealing procedure. Using the fabricated micro-rod resonators, single dissipative Kerr soliton microcombs are generated, and soliton repetition frequencies are tuned precisely by the iterative annealing process. The demonstrated method can be used for dual-comb spectroscopy and coherent optical communications.

Keywords: microcavities; nonlinear optics; pulse propagation; temporal solitons.

DOI: 10.3788/COL202119.071903

1. Introduction

Microresonators, which combine high quality (Q) factor and small mode volume, enhance light–matter interaction dramatically, making it an ideal platform to study nonlinear optical effects[1]. Various optical nonlinear effects have been observed and studied widely[2], among which the optical frequency comb (OFC) gains extensive attention for its compact size, low driving power, as well as high repetition frequency, and has been used in various new applications[3,4]. The dissipative Kerr soliton (DKS), which balances the loss of the optical resonator and parametric gain, along with dispersion and Kerr nonlinearity, is a special case of mode-locked OFC. Compared with general OFC, DKS provides better coherence and smooth envelope in the frequency domain, making it attractive for various areas[5]. By now, DKSs have been applied in optical clocks[6,7], ultralow-noise microwave generation[8,9], optical frequency synthesizers[10], and massively parallel coherent communication[11], just to name a few.

For decades, DKSs have been realized with various materials and machining techniques, with a repetition frequency ranging from several gigahertz (GHz) to terahertz (THz)[6]. In some applications such as dual-comb spectroscopy and massively parallel coherent communication, DKSs with similar repetition frequencies are essential. In dual-comb spectroscopy, the free spectral range (FSR) difference between the two generated DKS microcombs determines the signal-to-noise ratio of the down-converted RF spectrum[12]. Hence, a low FSR difference allows measurements using a low-frequency photodetector. In massively parallel optical communications, the repetition frequency difference between the DKS microcombs at the transmitter and receiver should be minimized to ensure the good performance of coherent detection. As the repetition frequency of DKS is determined by the FSR of resonator, the ability to control the FSR precisely is crucial. However, due to the compact size of microresonators, a slight fabrication error would result in a huge variation of the FSR. Thus, high-precision machining techniques have been employed to optimize the size of microresonators precisely. For instance, by using calibrated wet etching of the silica, a DKS repetition frequency difference of 2.6 MHz has been achieved with silica microresonators fabricated on a silicon wafer by a combination of lithography and wet/dry etching[13]. In Ref. [14], two soliton trains with a repetition frequency difference of 1.62 MHz are simultaneously generated in two different crystalline MgF_2 microresonators with FSR of about 12.1 GHz. In integrated photonic silicon nitride microresonators with FSR of about 100 GHz, the repetition frequencies of two DKSs generated by different microresonators are minimized through improving the uniformity of the fabrication process and thermal tuning, to avoid significant influence on the Q of the received signal[11]. In the micro-rod resonator, an external stress tuning method is demonstrated for precise and fast tuning of the repetition frequency of the DKS, with a tuning range of 30 MHz[15].

In this Letter, we present a novel method to control the FSR of silica micro-rod resonators precisely. Through the laser

annealing process, in which a CO_2 laser beam is employed to machine on the already-fabricated resonators for an appropriate duration, precise control of the FSR is realized, and the ultrahigh Q-factor is maintained. Single-DKS microcombs are generated in these FSR-optimized resonators after the iterative annealing process, and their repetition frequencies are measured to verify the effectiveness of the proposed method.

2. FSR Optimization with Laser Annealing

The so-called micro-rod resonators we employed were firstly, to the best of our knowledge, presented by the National Institute of Standards and Technology (NIST), which have the advantages of rapid fabrication and ultrahigh Q-factor[16]. The micro-rod resonators are fabricated by a CO_2 laser beam machining on a rotating silica rod. During the fabrication process, an annealing technology is applied to guarantee the ultrahigh Q-factor of the resonators. In the annealing process, the laser focus is placed slightly above the micro-rod resonator surface to ensure that the whole resonator surface gets heated evenly. Accompanied by the melting of glass, the resonator surface becomes smooth when assisted by the surface tension. To achieve the target FSR, the silica rod preform with corresponding diameter is selected as the platform to fabricate the resonator. The diameter of the silica rod can be changed by sweeping the CO_2 laser beam back and forth along the rod axis with enough laser power to get close to the target diameter. However, limited by the machining precision, the diameters of silica rod preforms are different initially. What is more, the accidental error induced by the runout accuracy of the motorized spindle and the movement accuracy of the motorized translation stages will also influence the fabrication reproducibility. All of these fabrication errors can make a random influence on the diameter of the fabricated resonator, thus preventing it from achieving an FSR difference of several megahertz (MHz).

Firstly, we investigated the fabrication errors of our resonator fabrication system through fabricating five resonators on a single silica rod preform successively. The resonators were fabricated with the same machining parameters. The diameter of the selected silica rod preform is about 3 mm, corresponding to an FSR of about 22 GHz. The shapes of the resonators' sidewalls are similar, as shown in the zoom-in photographs of two resonators in Fig. 1(a). As shown in Fig. 1(b), the FSRs of the five resonators range from 21.30 GHz to 21.23 GHz, indicating that the FSR variation is random and can be greater than 60 MHz. The result shows the typical FSR variation induced by fabrication errors. Meanwhile, as shown in Fig. 1(c), the Q-factors of these five resonators have also been measured and show a random characteristic. It is seen that the Q-factor of these resonators is about 1×10^8, which is necessary for DKS microcomb generation with relatively low power of the pump laser.

Therefore, to obtain identical resonators with similar FSR, it is necessary to remove the fabrication errors from already-fabricated resonators while the Q-factor is just slightly affected. To overcome this challenge, we propose to apply another laser

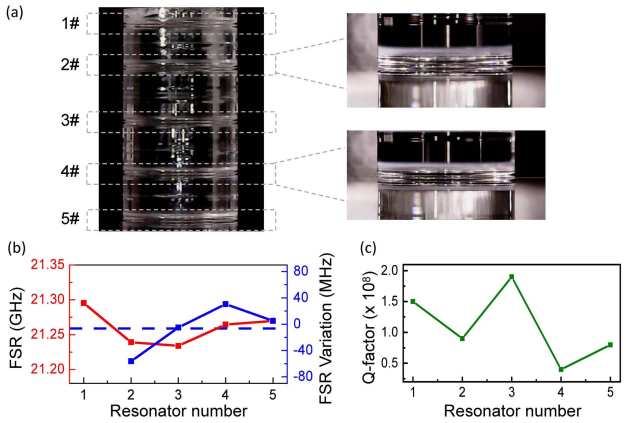

Fig. 1. (a) Photographs of the five micro-rod resonators fabricated on a single silica rod preform and the microscopy images of two resonators (2 and 4). (b) The FSRs and the FSR variation between every two resonators fabricated successively. (c) The Q-factors of the five fabricated resonators.

annealing process on already-fabricated resonators to realize a fine decrease of resonator diameter, just like we applied during the resonator fabrication process. Concretely, during the laser annealing process, the resonator surface is melted, and the shape of the resonator sidewall is changed with the volatilization of the silica. After the laser annealing process, the curvature of the resonator sidewall will be decreased slightly, inducing a fine decrease of resonator diameter. Eventually, by applying the laser annealing process iteratively, the FSR can be optimized to the target value. Importantly, in this method, the laser annealing time plays a key role in FSR tuning resolution. Theoretically, shorter annealing time can result in higher FSR tuning resolution and will be experimentally studied below.

To verify the feasibility of the proposed method, we conducted an experiment to optimize the FSR of an already-fabricated resonator repeatedly for up to five times, and the resonator is characterized after each annealing process. During the measurement, we kept the parameter of laser annealing process constant for every FSR optimizing process. Appropriate fabrication and coupling tactics were applied to excite just a few modes efficiently. Ordinarily, in the measurement, we focus on the cavity mode with maximum Q-factor value among all excited modes. Note that, after the laser annealing process, the excited mode spectrum will be slightly affected. To ensure that the cavity mode we focused can be excited, precise coupling and polarization adjustments were made after each annealing process. The annealing processes were repeated five times iteratively on the same resonator to verify its repeatability over a relatively long period of time. The transmission spectra for the resonator fabricated initially, annealed once, and annealed four times iteratively are shown in Figs. 2(a)–2(c), respectively. With the aforementioned measures, the spectral peaks of the target modes can be identified clearly in the transmission spectra, marked by black solid rectangles in Figs. 2(a)–2(c). A sideband technique was applied to ensure the FSR measuring accuracy[17]. As shown in Figs. 2(d)–2(f), the transmission spectra show three spectral peaks, as the two side peaks come from the phase modulation

sidebands that are coupled to the cavity through the initial neighboring cavity resonances. The modulation frequency f_m was set to be slightly less than the FSR, and FSR can be measured through the offset frequency as

$$\Delta f = \mathrm{FSR} - f_m. \tag{1}$$

As the modulation frequency generated with RF synthesizer is extremely precise, the measurement error of the FSR is mainly contributed by the measurement error of Δf, which can be minimized by using a Mach–Zehnder interferometer (MZI) as a reference spectrum. In the experiments, as the modulation frequency was set to a constant value of 21.8 GHz, the variation of the offset frequency equaled the FSR variation. As shown in Figs. 2(d)–2(f), the offset frequency increases with the increasing number of iterative annealing processes, meaning that the FSR is getting larger. The measured FSRs and FSR variation are shown in Fig. 2(g). The FSR nearly increases in a linear relationship with the number of iterative annealing processes. The average FSR variation is about 24.9 MHz, while its standard deviation can be calculated to be about 1.48 MHz, showing favorable repeatability.

Another thing we focused on is the impact on the Q-factor after the iterative annealing processes, as it will influence the threshold power for comb formation. As shown in Fig. 2(h), the Q-factor slightly fluctuates with the increase of the number of iterative annealing processes. It degrades by about 20% from the initial value, but still maintains an ultrahigh state. The equation of microresonator parametric oscillation threshold is given by[18]

$$P_{\mathrm{th}} \simeq 1.54 \frac{\pi}{2} \frac{\gamma_0 + \gamma_{c0}}{2\gamma_{c0}} \frac{n_0^2 \nu}{n_2 \lambda Q^2}, \tag{2}$$

where γ_0 is the internal decay rate of the cavity mode, γ_{c0} is the decay rate due to external coupling, n_0 is the refractive index of the material, n_2 is the nonlinearity coefficient of the material, ν is the mode volume, and λ is the resonant wavelength. In fact, as we discussed above, during the laser annealing process, only the Q-factor is slightly affected, while other resonator parameters almost hold fixed. So, the annealing process only gives slight negative impact on threshold power for comb formation. For example, as shown in Fig. 2(h), the Q-factor is degraded from 2.8×10^8 to 2.0×10^8, causing the threshold power to increase from 14 dBm to 17 dBm. Hence, the result shows that the microcomb can be generated with a relatively low pump power after the iterative annealing processes.

As mentioned above, the laser annealing time plays a key role in this method. To find out the highest precision of this method, we gradually reduced the annealing time from 30 to 10 s. For a certain annealing time, the annealing processes were repeated five times to minimize the influence of accidental errors, just as what we have performed in the experiments when annealing for 30 s. As the result shows in Fig. 3, the average FSR variation

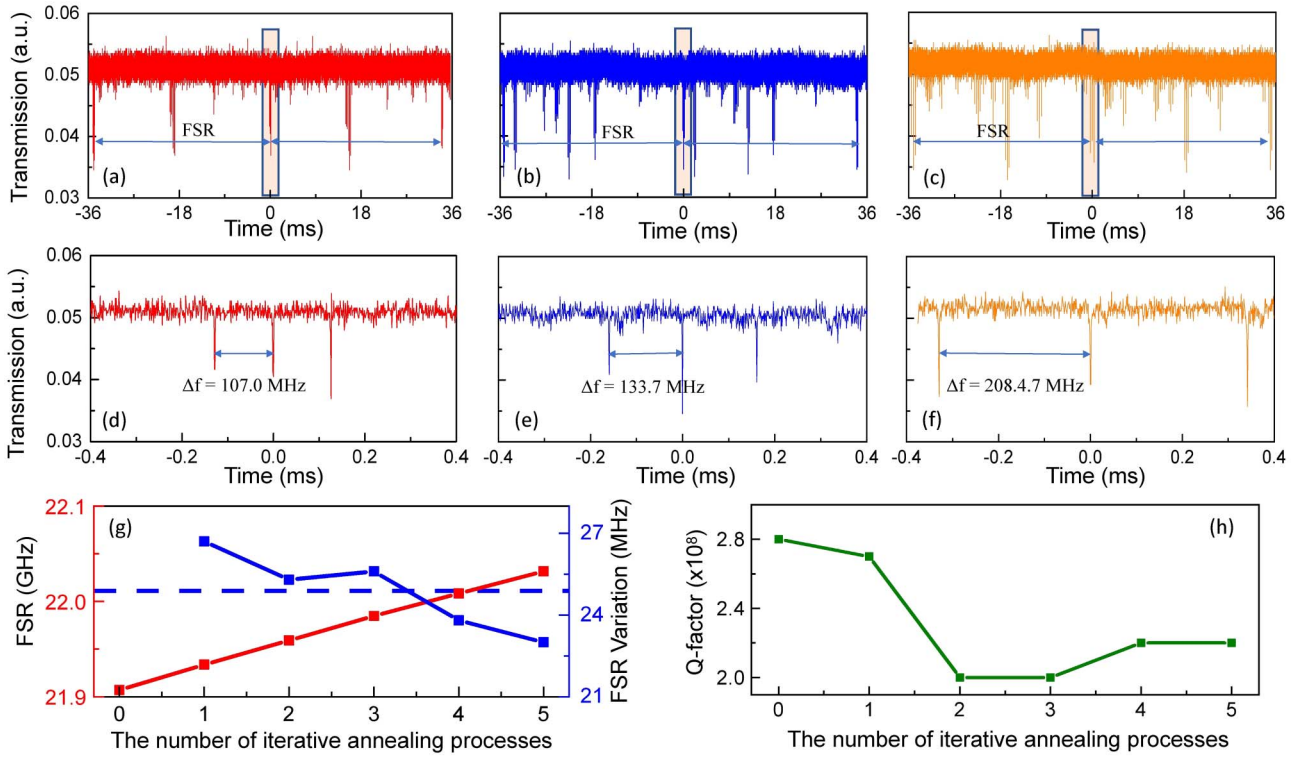

Fig. 2. (a)–(c) Transmission spectra of the resonator fabricated initially, annealed once, and annealed four times iteratively. The spectral peaks of the target modes are marked by black solid rectangles. The arrow lines mark the FSRs of the target modes. (d)–(f) Expanded plots of the spectral peaks of target modes, marked by black solid rectangles in (a)–(c). (g) The FSRs and the FSR variations vary with the number of iterative annealing processes. The dotted line represents the average value of FSR variation. (h) The Q-factor varies with the number of iterative annealing processes.

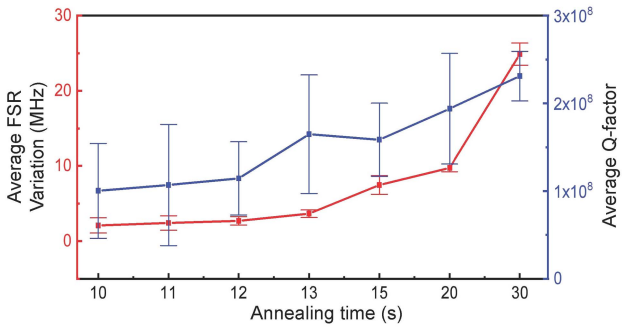

Fig. 3. Average FSR variation and average Q-factor vary with annealing time.

increases as the annealing time is lengthened. The minimum FSR variation is about 2.1 MHz with an annealing time of 10 s, while the maximum FSR variation is about 24.9 MHz with an annealing time of 30 s. The best resolution is smaller than 5 MHz, indicating that the FSR value (22 GHz) can be changed within 0.02%. The standard deviation of the FSR variation in experiments with different annealing times is below 1.5 MHz, verifying favorable stability and repeatability of the optimization method. On the other side, the impact on the Q-factor is also a matter of concern. For comparing the change trends with different annealing times, the initial resonators with a Q-factor of about 2.5×10^8 were fabricated in the experiments with different annealing times. It can be seen from Fig. 3 that the Q-factor decreases with the shortening of the annealing time. It can be explained as the worst melting uniformity of the resonator surface when annealing with a shorter time. The standard deviation of the Q-factor is remarkably smaller, with an annealing process of 30 s, than others, showing a better ability to maintain an ultra-high Q-factor. However, while the Q-factor is greater than 1×10^8 in most cases, the influence of larger standard deviation of the Q-factor is limited.

3. Soliton Generation Using Optimized Cavity

Precise control of resonator FSR is achieved by applying an iterative laser annealing process on already-fabricated resonators, and these optimized micro-rod resonators are ideal candidates for generating single-DKS with the target repetition frequency. Figure 4(a) gives the schematic of our experimental setup for soliton generation in resonators. An auxiliary laser heating method was adapted to overcome the thermal nonlinear effect of the microresonator and stably access single-DKS microcombs state[19]. In our experiment, we choose the same resonator mode (with the same wavelength) for both the pump and auxiliary lasers, but input them into the resonator from opposite directions. The pump and auxiliary lasers were from a narrow linewidth fiber laser, which can increase the stability of generated DKS microcombs. Two acoustic optical modulators with similar modulation frequency were utilized to access single-DKS

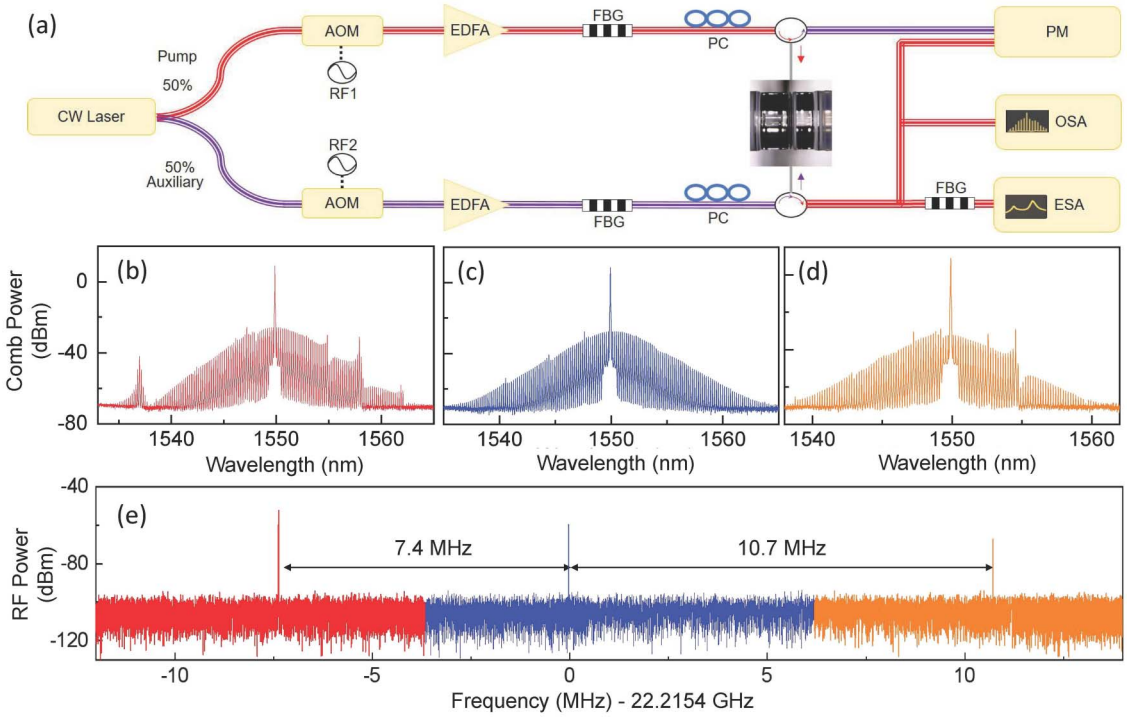

Fig. 4. (a) Experimental setup of single-DKS microcomb generation via auxiliary laser heating in micro-rod resonator. CW, continuous-wave narrow linewidth tunable fiber laser; AOM, acoustic optical modulator; EDFA, erbium-doped fiber amplifier; FPC, fiber polarization controller; FBG, fiber Bragg grating; PM, power measuring instrument; ESA, electrical spectrum analyzer; OSA, optical spectrum analyzer. (b)–(d) Optical spectra of the three single-DKS microcombs generated with a micro-rod resonator fabricated initially, annealed once, and annealed twice iteratively with 20 s annealing time. (e) RF beat note spectra of three single-DKS microcombs shown in (b)–(d).

microcombs state with high precision. The schematic of our experimental setup is shown in Fig. 4(a).

We conducted this experiment by using an optimized resonator with 20 s annealing process that characterized a 10 MHz resolution. The optical spectra of single-DKS generated in the resonator fabricated initially, annealed once, and annealed twice iteratively are presented in Figs. 4(b)–4(d). The three microcombs were generated with similar pump laser power of about 20 dBm, and the width of three optical DKS spectra covered a similar span of 25–30 nm around 1550 nm. The envelopes of the optical spectra in Figs. 4(b) and 4(d) show some imperfections, which are induced by avoided mode crossing[20]. The different spurs and dips in the three single-DKS spectra are the result of different excited modes, caused by the change of the shape of the resonator sidewall after the annealing process. The RF beat note spectra of the three single-DKS microcombs are shown in Fig. 4(e). The repetition frequency difference between the single-DKS microcombs generated with the resonators fabricated initially and annealed once is about 7.4 MHz, while the repetition frequency difference after annealing once and twice iteratively is about 10.7 MHz. In fact, the repetition frequency is also influenced by the pump frequency detuning. As the change in repetition frequency induced by the difference of pump frequency detuning is much smaller than 10 MHz[21], the measuring results of the repetition frequency can reflect the effect of our optimization method. By now, we have succeeded in optimizing the repetition frequency of the single-DKS microcomb generated with a micro-rod resonator with the precision of about 10 MHz.

4. Conclusion

In conclusion, we present a simple and effective method to control the FSR of micro-rod resonators precisely. We fabricated five resonators on a single silica rod preform firstly, to investigate the FSR variation caused by fabrication error, which indicated the order of magnitude of the FSR difference that needs to be optimized precisely. The optimization scheme was proposed, and the measuring method and feasibility were analyzed then. Afterward, the impacts of the annealing process with different durations on FSR variation and Q-factor were experimentally investigated. To verify its application potential, single-DKS microcombs were generated, and their repetition frequencies were measured. It has been proved that through the iterative laser annealing process, the repetition frequency of the generated single-DKS microcomb can be optimized with a precision of about 10 MHz. Our research results can extend the application scenarios of micro-rod resonators greatly.

Acknowledgement

This work was supported by the National Key Research and Development Program of China (No. 2019YFB2203103) and the National Natural Science Foundation of China (NSFC) (No. 61705033).

References

1. K. J. Vahala, "Optical microcavities," Nature **424**, 839 (2003).
2. Y. Li, X. Jiang, G. Zhao, and L. Yang, "Whispering gallery mode microresonator for nonlinear optics," arXiv:1809.04878 (2018).
3. W. Xu, C. X. Xu, F. F. Qin, Y. Q. Shan, Z. Zhu, and Y. Zhu, "Whispering-gallery mode lasing from polymer microsphere for humidity sensing," Chin. Opt. Lett. **16**, 081401 (2018).
4. K. W. Yang, H. L. Gong, X. L. Shen, Q. Hao, M. Yan, K. Huang, and H. P. Zeng, "Temperature measurement based on adaptive dual-comb absorption spectral detection," Chin. Opt. Lett. **18**, 051401 (2020).
5. T. J. Kippenberg, A. L. Gaeta, M. Lipson, and M. L. Gorodetsky, "Dissipative Kerr solitons in optical microresonators," Science **361**, 6402 (2018).
6. S. A. Diddams, T. Udem, J. C. Bergquist, E A. Curtis, R. E. Drullinger, L. Hollberg, W. M. Itano, W. D. Lee, C. W. Oates, K. R. Vogel, and D. J. Wineland, "An optical clock based on a single trapped $^{199}Hg^{+}$ ion," Science **293**, 825 (2001).
7. N. R. Newbury, "Searching for applications with a fine-tooth comb," Nat. Photon. **5**, 186 (2011).
8. T. M. Fortier, M. S. Kirchner, F. Quinlan, J. Taylor, J. C. Bergquist, T. Rosenband, N. Lemke, A. Ludlow, Y. Jiang, C. W. Oates, and S. A. Diddams, "Generation of ultrastable microwaves via optical frequency division," Nat. Photon. **5**, 425 (2011).
9. X. Xie, R. Bouchand, D. Nicolodi, M. Giunta, W. Hänsel, M. Lezius, A. Joshi, S. Datta, C. Alexandre, M. Lours, P. A. Tremblin, G. Santarelli, R. Holzwarth, and Y. Le Coq, "Photonic microwave signals with zeptosecond-level absolute timing noise," Nat. Photon. **11**, 44 (2017).
10. D. T. Spencer, T. Drake, T. C. Briles, J. Stone, L. C. Sinclair, C. Fredrick, Q. Li, D. Westly, B. R. Ilic, A. Bluestone, N. Volet, T. Komljenovic, L. Chang, S. H. Lee, D. Y. Oh, M. G. Suh, K. Y. Yang, M. H. P. Pfeiffer, T. J. Kippenberg, E. Norberg, L. Theogarajan, K. Vahala, N. R. Newbury, K. Srinivasan, J. E. Bowers, S. A. Diddams, and S. B. Papp, "An integrated-photonics optical-frequency synthesizer," Nature **557**, 81 (2018).
11. P. Marin-Palomo, J. N. Kemal, M. Karpov, A. Kordts, J. Pfeifle, M. H. Pfeiffer, P. Trocha, S. Wolf, V. Brasch, M. H. Anderson, R. Rosenberger, K. Vijayan, W. Freude, T. J. Kippenberg, and C. Koos, "Microresonator-based solitons for massively parallel coherent optical communications," Nature **546**, 274 (2017).
12. T. Ideguchi, S. Holzner, B. Bernhardt, G. Guelachvili, N. Picqué, and T. W. Hänsch, "Coherent Raman spectro-imaging with laser frequency combs," Nature **502**, 355 (2013).
13. M.-G. Suh, Q. Yang, K. Yang, X. Yi, and K. J. Vahala, "Microresonator soliton dual-comb spectroscopy," Science **354**, 600 (2016).
14. N. G. Pavlov, G. Lihachev, S. Koptyaev, E. Lucas, M. Karpov, N. M. Kondratiev, I. A. Bilenko, T. J. Kippenberg, and M. L. Gorodetsky, "Soliton dual frequency combs in crystalline microresonators," Opt. Lett. **42**, 514 (2017).
15. R. Niu, S. Wan, S. M. Sun, T. G. Ma, H. J. Chen, W. Q. Wang, Z. Z. Lu, W. F. Zhang, G. C. Guo, and C. L. Zou, "Repetition rate tuning of soliton in microrod resonators," arXiv:1809.06490 (2018).
16. P. Del'Haye, S. A. Diddams, and S. B. Papp, "Laser-machined ultra-high-Q microrod resonators for nonlinear optics," Appl. Phys. Lett. **102**, 221119 (2013).
17. J. Li, H. Lee, K. Y. Yang, and K. J. Vahala, "Sideband spectroscopy and dispersion measurement in microcavities," Opt. Express **20**, 26337 (2012).
18. A. B. Matsko, A. A. Savchenkov, D. Strekalov, V. S. Ilchenko, and L. Maleki, "Optical hyperparametric oscillations in a whispering-gallery-mode resonator: threshold and phase diffusion," Phys. Rev. A **71**, 033804 (2005).
19. H. Zhou, Y. Geng, W. Cui, S. Huang, Q. Zhou, K. Qiu, and C. Wong, "Soliton bursts and deterministic dissipative Kerr soliton generation in auxiliary-assisted microcavities," Light: Sci. Appl. **8**, 1 (2019).
20. T. Herr, V. Brasch, J. Jost, I. Mirgorodskiy, G. Lihachev, M. Gorodetsky, and T. Kippenberg, "Mode spectrum and temporal soliton formation in optical microresonators," Phys. Rev. Lett. **113**, 123901 (2014).
21. C. Bao, P. Liao, A. Kordts, M. Karpov, M. H. Pfeiffer, L. Zhang, Y. Cao, G. Xie, C. Liu, Y. Yan, A. Almaiman, A. Mohajerin-Ariaei, A. Fallahpour, M. Tur, T. J. Kippenberg, and E. Willner, "Soliton repetition rate in a silicon-nitride microresonator," Opt. Lett. **42**, 759 (2017).